Hepsin promotes prostate cancer progression and metastasis

Olga Klezovitch,[1,4] John Chevillet,[1,2,4] Janni Mirosevich,[3] Richard L. Roberts,[3] Robert J. Matusik,[3] and Valeri Vasioukhin[1,*]

[1]Division of Human Biology, Fred Hutchinson Cancer Research Center, Seattle, Washington, 98109
[2]Molecular and Cellular Biology Program, University of Washington, Seattle, Washington, 98195
[3]Department of Urologic Surgery, Vanderbilt Prostate Cancer Center, Department of Cancer Biology, Vanderbilt-Ingram Cancer Center, Vanderbilt University Medical Center, Nashville, Tennessee 37232
[4]These authors contributed equally to this work.
*Correspondence: vvasiouk@fhcrc.org

Summary

The majority of cancer-related deaths are associated with metastasis; however, little is known about the mechanisms of this process. Hepsin is a cell surface serine protease that is markedly upregulated in human prostate cancer; however, the functional significance of this upregulation is unknown. We report here that hepsin overexpression in prostate epithelium in vivo causes disorganization of the basement membrane. Overexpression of hepsin in a mouse model of nonmetastasizing prostate cancer has no impact on cell proliferation, but causes disorganization of the basement membrane and promotes primary prostate cancer progression and metastasis to liver, lung, and bone. We provide in vivo evidence that upregulation of a cell surface serine protease in a primary tumor promotes cancer progression and metastasis.

Introduction

Extracellular and cell surface proteases play an important role in development and normal tissue homeostasis (Werb et al., 1999). In addition, these enzymes are believed to be especially important during the final stages of primary tumor progression, invasion, and metastasis. It is hypothesized that they are involved in the cleavage of extracellular matrix proteins to allow tumor cells to invade the connective tissues, blood, and lymph vessels and subsequently travel out of the vasculature to distant sites. While multiple types of proteases are involved in these activities, most of the attention in previous years has been devoted to the matrix metalloproteinases (MMPs) (Chang and Werb, 2001). In addition to MMPs, serine proteases have been implicated in degradation of the extracellular matrix and modulation of cell-substratum adhesion in tumor cells (Del Rosso et al., 2002). Type II transmembrane serine proteases represent a specialized group of cell surface proteolytic enzymes (Hooper et al., 2001). The C-terminal serine protease domain of these proteins is localized at the cell surface and interacts with extracellular matrix components and transmembrane molecules. The N-terminal cytoplasmic domain associates with intracellular molecules and participates in signaling. While the functional role of these enzymes is largely unknown, interest in these molecules stems from observations that they are often overexpressed in cancer.

Several recent DNA microarray studies of gene expression in human prostate carcinomas have revealed marked overexpression of hepsin, a type II transmembrane serine protease (Chen et al., 2003; Dhanasekaran et al., 2001; Ernst et al., 2002; Luo et al., 2001; Magee et al., 2001; Stamey et al., 2001; Stephan et al., 2004; Welsh et al., 2001). Hepsin mRNA is upregulated in 90% of prostate tumors, with levels often increased $>$10 fold, and exclusively expressed in tumor cells. Upregulation of hepsin RNA levels was accompanied by an increase in protein levels (Dhanasekaran et al., 2001). It is not clear how hepsin mRNA levels correlate with different stages/grades of prostate cancer. Although initial studies showed that hepsin levels were highest in prostatic intraepithelial neoplasia (PIN) and decrease with prostate cancer progression (Dhanasekaran et al., 2001), other studies have demonstrated that hepsin mRNA levels increase with prostate cancer progression and reach maximum levels in more advanced (Gleason grade 4/5) prostate carcinomas (Chen et al., 2003; Stamey et al., 2001). At present, it is unclear if overexpression of hepsin in prostate cancer cells plays a role in prostate cancer development or progression, and what mechanisms may be responsible for this role.

To determine the role of hepsin in prostate epithelium in vivo, we generated and analyzed probasin promoter-driven hepsin transgenic mice (PB-hepsin). We found that hepsin overexpression causes weakening of epithelial-stromal adhesion. Immunofluorescent staining and electron microscopy revealed the disor-

SIGNIFICANCE

Knowledge about the mechanisms responsible for metastasis is pivotal for development of efficient therapies to combat cancer. Here we demonstrate that hepsin, a cell surface protease that is markedly upregulated in human prostate cancer, promotes prostate cancer progression and metastasis. Upregulation of hepsin causes disorganization and disruption of the prostate basement membrane, and this may be the mechanism by which hepsin promotes metastasis. Our findings suggest that the development of therapeutic approaches to specifically inhibit hepsin proteolytic activity may provide a valuable tool to decrease metastasis in prostate cancer patients.

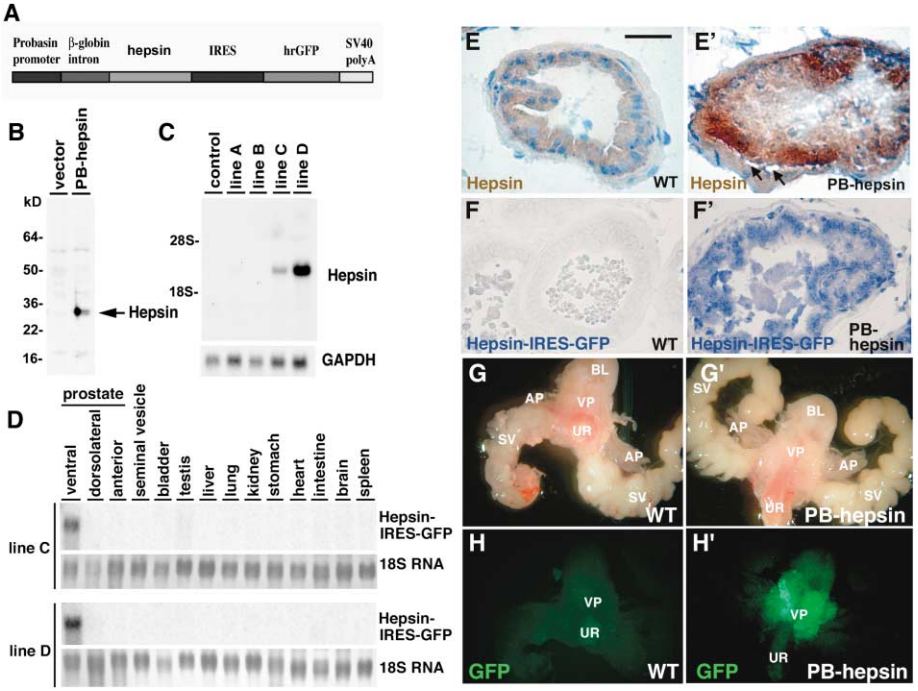

Figure 1. Generation of transgenic mice overexpressing hepsin in prostate epithelium

A: Schematic representation of probasin-hepsin (PB-hepsin) transgene.

B: The PB-hepsin transgenic construct produces hepsin protein in a prostate carcinoma cell line. The empty vector or PB-hepsin construct was transiently transfected into LNCaP cells and total protein extracts were analyzed by Western blot with anti-hepsin antibodies.

C: The PB-hepsin transgenic mouse lines C and D express hepsin mRNA in the prostate gland. Total RNA was extracted from the prostate glands of 10-week-old control (control) and transgenic (lines A–D) mice and analyzed by Northern blot hybridization using hepsin and GAPDH probes.

D: Ventral prostate-specific expression of the PB-hepsin transgene. Total RNA was extracted from indicated prostate lobes and organs of 21-week-old PB-hepsin animals (line C and D) and analyzed by Northern blot hybridization with GFP (Hepsin-IRES-GFP) and 18S RNA probes.

E and E′: Immunohistochemical staining of 14-week-old wild-type (WT) and PB-hepsin prostate glands with anti-hepsin antibodies. Arrows indicate areas of separation between the epithelial and stromal cell compartment.

F and F′: In situ hybridization of ventral prostates from the 14-week-old animals with antisense hrGFP probe.

G–H′: Macroscopic appearance and GFP-imaging of selected urogenital organs from wild-type and PB-hepsin animals. Bladders (BL) with urethras (UR), seminal vesicles (SV), and anterior (AP) and ventral (VP) prostate lobes were dissected from 20-week-old wild-type (**G** and **H**) and PB-hepsin (**G′** and **H′**) animals. The organs were visualized using visible light (**G** and **G′**) and GFP fluorescence (**H** and **H′**). Note prominent GFP fluorescence in the ventral prostate lobes of PB-hepsin mice.

Bar in **E** represents 55 μm in **E–F′**.

ganization and disruption of the basement membrane in hepsin-expressing prostate glands. To determine the potential role of hepsin in prostate cancer progression, we crossed PB-hepsin transgenic animals with mice expressing the SV40 large T antigen in the prostate epithelium (LPB-Tag mice, line 12T-7f) (Kasper et al., 1998). LPB-Tag animals develop PIN lesions and foci of prostate carcinoma; however, primary tumors do not metastasize. We found that by 21 weeks of age, up to 55% of the double transgenic LPB-Tag/PB-hepsin mice, but none of the single transgenic LPB-Tag or PB-hepsin animals, develop prostate cancer that metastasizes to liver, lung, and bone. These data indicate that hepsin promotes primary prostate cancer progression and metastasis in the LBP-Tag mouse model of prostate cancer.

Results

Generation of transgenic mice expressing hepsin in prostate epithelium

The modified probasin promoter (ARR_2PB) is specifically active in prostate epithelial cells in vivo and in vitro and was used for prostate-specific expression of hepsin (Zhang et al., 2000). In addition to the promoter, the transgenic construct contains the β-globin intron, full-length mouse hepsin cDNA, internal ribosome entrance site (IRES), and humanized *renilla* GFP (hrGFP) cDNA sequences (Figure 1A). This configuration directs the expression of hepsin and hrGFP proteins from the same transcript, allowing for convenient monitoring of transcription specificity by whole-mount internal organ GFP detection (Figures 1G–1H′).

To confirm the functionality of the transgenic construct, LNCaP human prostate carcinoma cells were transiently transfected with the probasin-hepsin (PB-hepsin) plasmid. Western blot analysis of total protein extract from hepsin-transfected cells using anti-hepsin antibodies revealed a 31 kDa band corresponding to the heavy chain of proteolytically processed hepsin (Figure 1B). Four mouse lines transmitting the PB-hepsin transgene were generated and analyzed. Northern blot hybridization with hepsin probe revealed that only two lines (C and D) expressed the transgene (Figure 1C). The expression of the transgene was restricted to the ventral lobe of the prostate gland, and it was not detectable in other organs and tissues (Figure 1D). Similar data were obtained using RT-PCR analysis (data not shown, 3 animals were analyzed for each line). Since endogenous hepsin expression was not detected in the prostates of wild-type 10-week-old animals, it is difficult to estimate how the levels of hepsin in our transgenic animals correspond to the levels of hepsin in human prostate cancer, where hepsin transcripts are upregulated up to 34-fold in comparison to normal tissue (Stamey et al., 2001).

Immunohistochemical staining with anti-hepsin antibodies ($n = 2$) and in situ hybridization with an antisense GFP probe ($n = 3$) demonstrated prostate epithelial cell specific expression of the transgene (Figures 1E–1F′). To establish whether the transgenic construct also expressed functional hrGFP protein, whole-mount internal organ GFP detection was performed using a dissecting microscope with GFP attachment (Figures 1G–1H′). The hrGFP expression was readily detectable in the ventral lobe of prostate gland of the PB-hepsin animals ($n > 30$). Although

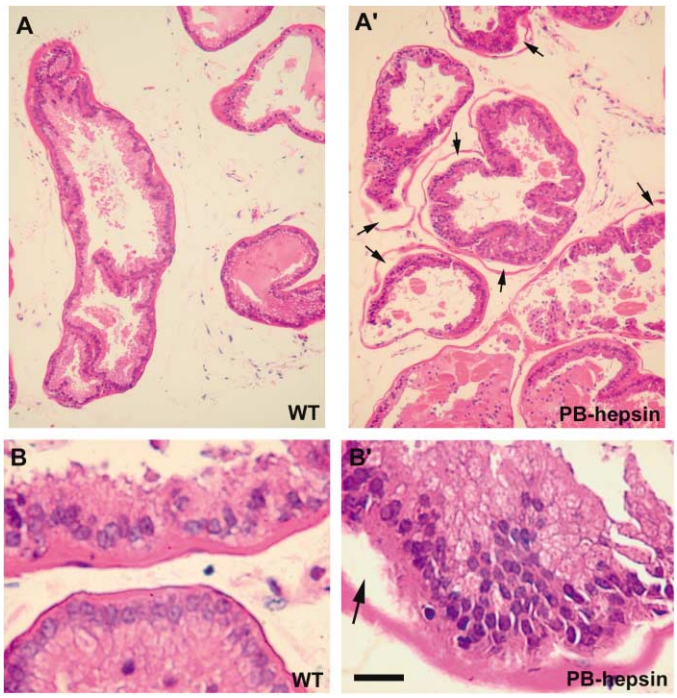

Figure 2. Histologic appearance of ventral prostate lobes from control (WT) and PB-hepsin (PB-hepsin) animals

Tissue sections were stained with hematoxylin and eosin and examined using 10× (**A** and **A′**) and 40× (**B** and **B′**) objectives. Note separation between epithelial cells and the stromal layer in the PB-hepsin animals (arrows in **A′** and **B′**). Bar in **B′** represents 120 μm in **B** and **B′**.

GFP fluorescence was visible by whole-mount organ GFP analysis, expression was too weak to be detected on frozen tissue sections (data not shown). This enabled us to use the green channel for detection of other proteins in triple immunofluorescence staining during analysis of the PB-hepsin mice (see below).

PB-hepsin transgenic mice undergo normal differentiation, proliferation, and apoptosis, but display disorganization of the basement membrane

Histologic examination of prostates from 3- to 4-month-old animals revealed no obvious abnormalities in the prostate glands of PB-hepsin transgenic mice (data not shown). In contrast, 3 out of 4 one-year-old PB-hepsin, but none of the control, littermates (n = 5) displayed separation between the epithelial and stromal cell layers (arrows in Figures 2A–2B′). Small areas of separation between the epithelial and stromal cell layers were occasionally observed in the younger 14-week-old PB-hepsin mice (3 of 7 mice). These areas coincide with the epithelial fragments expressing high levels of hepsin (arrows in Figure 1E′). While it is likely that separation was induced by the fixation and sectioning procedures, these results suggest a weakening of epithelial-stromal adhesion in the PB-hepsin animals.

The epithelial and stromal cell compartments of the prostate are separated by the basement membrane, which is composed of numerous extracellular matrix proteins produced by both stromal and epithelial cells (Nagle et al., 1995). Since epithelial-stromal adhesion is compromised in PB-hepsin mice, we analyzed localization of cell-substratum adhesion proteins. This study utilized 4- to 5-month-old mice, a time point before the manifestation of the massive defects in epithelial-stromal adhesion observed in older animals. To analyze whether the expression of hepsin in transgenic mice affected the basement membrane, immunofluorescence staining was performed with antibodies against the basement membrane markers Laminin 5 (Laminin γ 2) and Collagen IV. In wild-type littermates, Laminin 5 staining appeared as a continuous line separating the stromal and epithelial cell compartments (arrows in Figure 3A, n = 5). In contrast, Laminin 5 staining in PB-hepsin transgenic mice appeared weak or completely absent (Figure 3A′, n = 5). Antibodies against Collagen IV revealed disorganized and diffuse localization of this protein in PB-hepsin prostates (Figure 3B′, n = 4). Although the basement membrane displayed normal focal staining, generally the staining appeared fragmented, with large sections of the epithelial-stromal interface devoid of Collagen IV. This pattern of Laminin 5 and Collagen IV localization indicated a perturbation of the basement membrane in the PB-hepsin transgenic animals.

One of the major basement membrane receptors expressed in the prostate epithelium is α6β4-integrin, which is associated with hemidesmosomes. Expression of β4-integrin is decreased in human prostate carcinoma (Bonkhoff, 1998; Davis et al., 2001; Murant et al., 1997). Immunofluorescence staining with anti-β4-integrin antibodies revealed perturbation of the hemidesmosomal organization in the PB-hepsin prostates. Wild-type mice displayed a continuous line of β4-integrin staining along the basement membrane (arrows in Figure 3C, n = 5). In contrast, the β4-integrin staining in the transgenic prostate appeared as a discontinuous line (Figure 3C′, n = 5), similar to the "beads on a string" appearance of β4-integrin in the skin of Laminin 5-deficient mice (Ryan et al., 1999). Taken together, the immunofluorescence staining with markers of the basement membrane and cell-substratum adhesion structures suggests that the integrity of the basement membrane is severely compromised in PB-hepsin transgenic animals.

Prostate epithelium contains two major cell populations: basal cells, which are characterized by the keratin 5/14 expression, and luminal cells, which are characterized by keratin 8/18 expression. To determine whether perturbation of the basement membrane in the PB-hepsin transgenic mice impacted normal prostate epithelial cell differentiation, we performed immunofluorescent staining with a variety of cell type-specific markers. Staining with markers of basal and luminal cells revealed that both cell types are present in the PB-hepsin transgenic animals (Figures 3D and 3D′). The basal cells represented 12.76 ± 0.73% of total basal and luminal epithelial cells in the wild-type (n = 3) and 12.36% ± 1.64% in the PB-hepsin transgenic animals (n = 3). We conclude that upregulation of hepsin in prostate epithelium did not lead to changes in cell differentiation.

Cell-substratum adhesion is important for regulation of cell proliferation and cell survival. While upregulation of hepsin had no impact on overall size of the prostate gland in the transgenic animals (data not shown), it was necessary to determine whether hepsin causes differences in proliferation or cell death. To identify proliferating cells, immunostaining with anti-Ki67 antibody was performed. We found that only a very small proportion of epithelial cells (0.1%–0.2%) were proliferating in control wild-type prostates (Figure 3E, n = 3). Upregulation of hepsin had no impact on the number of Ki67-positive cells (Figure 3E′, n = 3).

To determine whether hepsin overexpression leads to

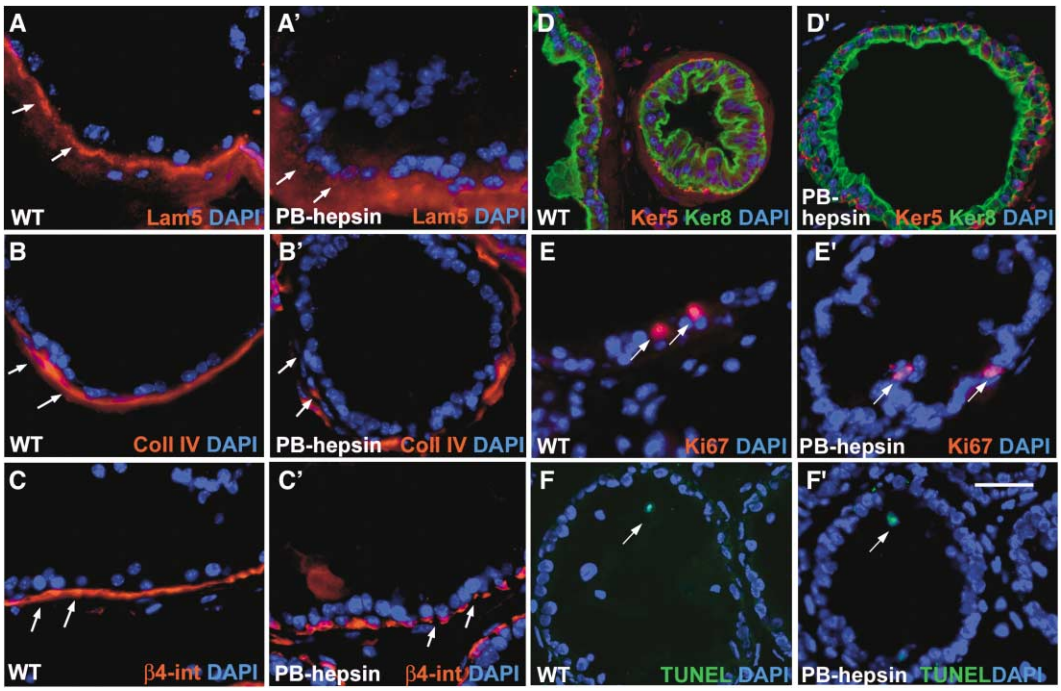

Figure 3. Perturbation of the basement membrane, but maintenance of normal differentiation, proliferation, and apoptosis, in the prostate glands of PB-hepsin transgenic mice

Immunofluorescent staining of ventral prostate glands from 14-week-old wild-type (WT) and PB-hepsin (PB-hepsin) transgenic mice with anti-Laminin 5 (**A** and **A′**), anti-Collagen IV (**B** and **B′**), anti-β4-integrin (**C** and **C′**), and anti-Ki67 (Ki67) (**E** and **E′**) antibodies, and TUNEL staining for apoptotic cells (**F** and **F′**). Double immunofluorescent staining with anti-keratin 5 (Ker5, shown in red) and anti-keratin 8 (Ker8, shown in green) antibodies (**D** and **D′**). White arrows in **A**–**C′** show the position of the basement membrane. DAPI-stained nuclei are shown in blue. The scale bar in **F′** represents 35 μm.

changes in programmed cell death, we performed TUNEL staining (Figures 3F and 3F′). Few epithelial cells in the wild-type prostate (0.02%–0.05%) were TUNEL-positive, and these were usually localized to the lumen of the prostatic acinus (n = 3). The numbers and localization of apoptotic cells were similar in the PB-hepsin animals (n = 3). We conclude that overexpression of hepsin in prostate epithelia did not lead to changes in cell proliferation or apoptotic cell death.

Ultrastructural abnormalities in the prostate basement membrane in PB-hepsin transgenic animals

To determine which part of the epithelial-stromal adhesion system is affected in hepsin-expressing prostates, 14-week-old transgenic animals were analyzed using transmission electron microscopy (Figures 4A and 4B′). Although the overall ultrastructure of prostates from PB-hepsin transgenic mice is similar to that of the wild-type controls, the organization of the basement membrane is consistently affected in the PB-hepsin animals (Figure 4A′). The basement membrane in the wild-type animals contains tightly packed collagen fibers (Figure 4B, n = 2). Microblisters separating the epithelial and stromal cell compartments are abundantly present in the transgenic animals. High magnification images of the blisters show disruption of the structure at the level of basement membrane (Figure 4B′, n = 2). Collagen fibers were present in the basement membrane of PB-hepsin prostates; however, the adhesion between the fibers appears to be compromised. While it is likely that microblisters were induced by stress during fixation and sectioning procedures, the microblistering indicates a failure of proper adhesion between collagen fibers in the basement membrane of the PB-hepsin animals.

Hepsin promotes prostate cancer progression

In human prostate cancer progression, disruption of the basement membrane occurs during the transition from carcinoma in situ to invasive, metastasizing carcinoma (Abate-Shen and Shen, 2000). To determine the significance of hepsin-mediated disruption of the basement membrane in prostate cancer, we utilized the LPB-Tag (Line 12T-7f) mouse model of prostate cancer (Kasper et al., 1998). LPB-Tag mice express the SV40 large T antigen (Tag) under the control of the probasin promoter, which directs expression of the transgene specifically to the prostatic epithelium and accessory sex glands. The males of this transgenic line develop high-grade PIN and limited foci of adenocarcinoma at 20 weeks of age, but do not develop metastases. We first analyzed whether endogenous hepsin is upregulated in the prostate of the LPB-Tag animals. Northern blot analysis with a hepsin probe revealed no detectable endogenous hepsin expression in these animals (Figure 5G, n = 2).

To determine the role of hepsin in prostate cancer, we generated and analyzed double transgenic LPB-Tag/PB-hepsin mice. The LPB-Tag animals were crossed with the two independently generated lines of PB-hepsin mice (lines C and D), and double transgenic LPB-Tag/PB-hepsin males were analyzed at 21 weeks after birth. As previously reported, the LPB-Tag animals display massive enlargement of the prostate gland. The double transgenic LPB-Tag/PB-hepsin animals also showed enlargement of the prostate that was similar in size and weight to the

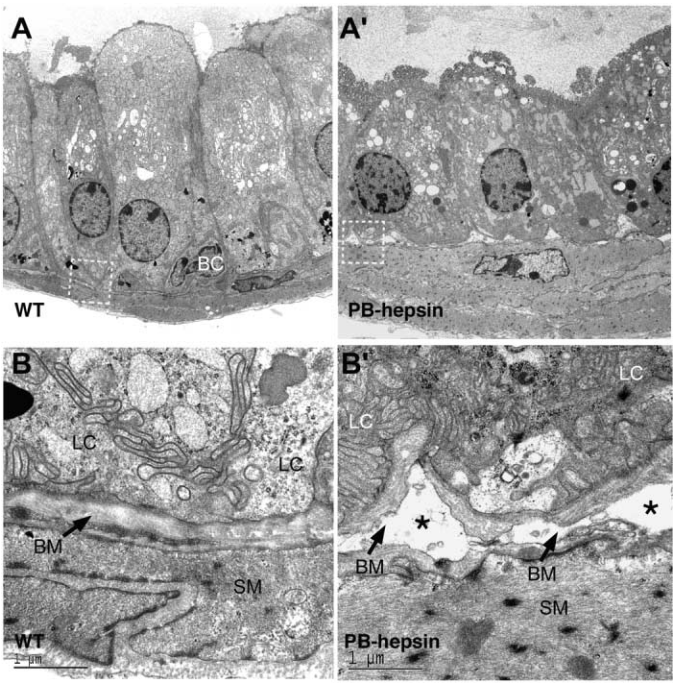

Figure 4. Ultrastructural analysis of ventral prostates

Ultrastructural analysis of ventral prostates from 14-week-old male wild-type (**A** and **B**) and PB-hepsin (**A′** and **B′**) transgenic mice. Areas within the dashed square of **A** and **A′** are shown at higher magnification in **B** and **B′**, respectively. The basement membrane in wild-type prostates is structurally intact and is tightly packed with collagen fibers (arrow in **B**). Transgenic prostates display microblisters at the basement membrane (shown with asterisk in **B′**). BM, basement membrane; SM, smooth muscle cell in the stromal cell compartment; LC, luminal cell; BC, basal cell. Bar in **B′** represents 1 μm in **B** and **B′**, and 7 μm in **A** and **A′**.

prostates from LPB-Tag animals (data not shown). Histologic examination of prostate glands from LPB-Tag animals revealed typical PIN-like lesions and stromal cell hyperplasia (Figures 5A and 5B, n = 15). The prostate glands from the LPB-Tag/PB-hepsin animals display areas showing disruption and disorganization of epithelial structure (Figures 5A′ and 5B′, n = 26). In addition to PIN-like lesions, prostates from LPB-Tag/PB-hepsin double mutant mice typically showed adenocarcinoma with extensive glandular differentiation and focal areas of "punched out," cribriform lesions. Often, the neoplastic glands invaded the periprostatic stroma (arrow in Figure 5B′). In half of the analyzed double transgenic mice, the tumor cells showed nuclear and chromatin patterns as well as architectural features including "rosette formation" that suggested neuroendocrine (NE) differentiation (arrowhead in Figure 5B′). These changes were not due to the differences in the levels of SV40 T antigen, which were found to be similar between the LPB-Tag and LPB-Tag/PB-hepsin prostates (Figure 5H).

Staining with Ki67 antibodies revealed no difference in cell proliferation between the prostates of LPB-Tag and LPB-Tag/PB-hepsin animals (Figures 5C and 5C′, I, n = 3). In contrast, TUNEL staining showed a 4-fold increase in apoptosis in the double transgenic animals (Figures 5D, 5D′, and 5J, n = 4).

To determine whether hepsin expression causes changes in the organization of the basement membrane in this model, we performed immunofluorescent staining with antibodies recognizing extracellular matrix proteins. We found that Laminin 5 was absent in both LPB-Tag and LPB-Tag/PB-hepsin prostates (data not shown). Collagen IV staining was severely reduced in the hepsin-expressing prostates (Figures 5E and 5E′, n = 2). In addition, β4-integrin staining revealed disorganization and disruption of basement membrane receptors in the LPB-Tag/PB-hepsin double transgenic animals (Figures 5F and 5F′, n = 3). These changes in staining pattern were similar to changes found in PB-hepsin animals, suggesting hepsin-mediated disorganization of the basement membrane in the LPB-Tag mouse model of prostate cancer. Since cell-substratum adhesion is an important source of cell survival signals, the increase in apoptosis in the LPB-Tag/PB-hepsin animals may be a consequence of the disorganization of the basement membrane, which provides major ligands for cell adhesion receptors.

Hepsin promotes prostate cancer metastasis

Animals from the LPB-Tag 12T-7f line do not display prostate cancer metastases (Kasper et al., 1998). In contrast, by 21 weeks of age, up to 55% of double transgenic LPB-Tag/PB-hepsin mice developed prominent metastasis (Table 1, Figure 6). LPB-Tag/PB-hepsin animals obtained using two independently generated PB-hepsin lines developed metastases, confirming that metastasis was due to hepsin upregulation and not the site of transgene integration. Metastases were observed in the liver, lung, and bone of the LPB-Tag/PB-hepsin transgenic animals (Table 2). RNA extracted from the livers and lungs of LPB-Tag/PB-hepsin mice was positive for PB-hepsin transcripts (Figure 6B). In addition, PB-hepsin mRNA was detectable in the bone metastases by in situ hybridization (Figure 6I, n = 2). These data demonstrate active hepsin expression in the metastatic lesions. Immunohistochemical analysis demonstrated that metastases were also positive for androgen receptor and SV40 large T antigen, confirming their prostatic origin (arrows in Figures 6J and 6L, n = 4). Metastatic lesions in other SV40 T antigen-driven mouse models of prostate cancer (TRAMP, CR2-T-Ag, LPB-Tag line 12-T10) display features of NE differentiation (Shappell et al., 2004). Morphologically, metastases in LPB-Tag/PB-hepsin animals contained tightly packed cells displaying nuclear molding and high nuclear/cytoplasmic ratio that was consistent with features of NE differentiation. Moreover, these metastatic lesions were positive for synaptophysin, a marker of NE cells, confirming their NE differentiation (Figure 6K, n = 4). Overall, we conclude that upregulation of hepsin in a mouse model of prostate cancer resulted in marked progression of prostatic tumors and caused the development of NE metastatic tumors to the liver, lung, and bone.

Discussion

The metastatic cascade is a complex process consisting of a number of important steps that include loss of tissue architecture, local invasion, invasion into blood and lymph vessels, extravasation, establishment of the secondary foci, and angiogenesis (Robinson et al., 2004). Failure to complete any of these steps would result in the absence of metastases. The classic model of the metastatic process assumes that metastases arise from the rare cells that, in addition to the early oncogenic alteration enabling them to form primary tumor, subsequently accumulated novel mutations that promote metastasis.

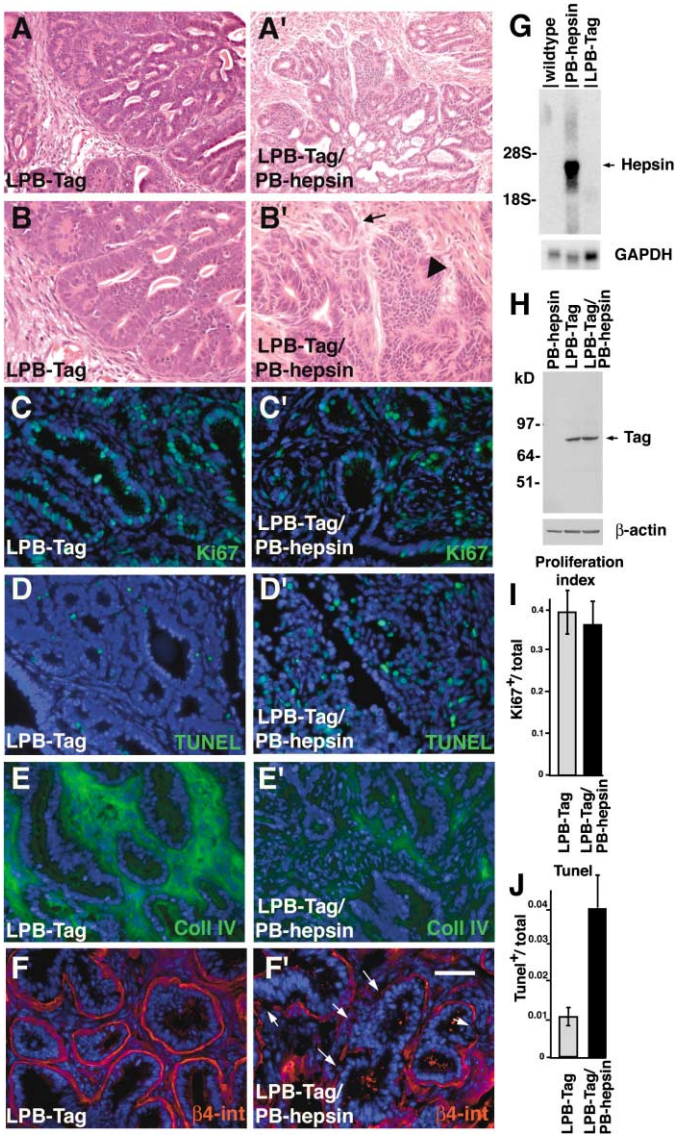

Figure 5. Hepsin causes disruption of epithelial structure and promotes cancer progression in the SV40 T antigen-driven mouse model of prostate cancer

A–B′: Histologic appearance of ventral prostates from 21-week-old LPB-Tag and LPB-Tag/PB-hepsin animals. Note disorganization of epithelial structure, adenocarcinoma with glandular differentiation, and foci of poorly differentiated NE adenocarcinoma (arrowhead in **B′**) in LPB-Tag/PB-hepsin animals.
C and **C′**: Immunostaining with anti-Ki67 antibodies shows no differences in cell proliferation between LPB-Tag and LPB-Tag/PB-hepsin animals.
D and **D′**: Apoptosis is increased in the prostates of LPB-Tag/PB-hepsin mice. Apoptotic cells were detected using TUNEL staining (green).
E and **E′**: Decreased staining for Collagen IV in LPB-Tag/PB-hepsin mice (green).
F and **F′**: Immunostaining with anti-β4-integrin antibodies (red) reveals disorganization of basement membrane receptors in LPB-Tag/PB-hepsin mice (arrows).
G: Endogenous hepsin is not upregulated in the prostate of LPB-Tag mice. RNA was extracted from ventral prostates of wild-type, PB-hepsin, and LPB-Tag animals and analyzed by Northern blot hybridization with hepsin and GAPDH probes.
H: Absence of changes in the levels of T-antigen (Tag) in LPB-Tag/PB-hepsin animals. Proteins from ventral prostates of PB-hepsin, LPB-Tag, and LPB-tag/PB-hepsin animals were analyzed by Western blotting with anti-Tag and anti-β-actin antibodies.
I: Quantitation of the experiments shown in **C** and **C′**. Proliferation index determined as a ratio of proliferating cells ($Ki67^+$) to the total cell number.
J: Quantitation of experiments shown in **D** and **D′**. Number of $TUNEL^+$ cells per total cell numbers was counted. Note that staining with FITC-labeled secondary antibodies was possible because hrGFP fluorescence was too weak to be detected on frozen tissue sections (data not shown).
The scale bar in **F′** represents 66 μm for frames **A** and **A′**, and 33 μm for **B–F′**.

The recently proposed alternative model suggests that combination of early oncogenic alterations in the primary tumor determines its metastatic potential (Bernards and Weinberg, 2002). We have found that hepsin has no impact on cell proliferation and, therefore, it does not act as a classic oncogene. In contrast, increase in hepsin expression leads to disorganization of the basement membrane and promotes primary prostate cancer progression and metastasis. These hepsin functions are consistent with the classic model of metastatic process. On the other hand, the fact that hepsin becomes upregulated very early in the human prostate cancer at the stage of PIN-like lesions is more in line with the alternative model of metastasis. Therefore, it appears that our findings provide some support for both models. It is possible that some middle ground may exist between these seemingly opposing views of metastatic process.

The basement membrane is a specialized extracellular matrix structure that separates the epithelial and stromal cell compartments. Loss of the basement membrane is a mandatory step that occurs during local invasion early in the metastatic process (Abate-Shen and Shen, 2000; Robinson et al., 2004). To accomplish local invasion, tumor cells use extracellular and cell surface proteolytic enzymes to degrade the basement membrane proteins (Chang and Werb, 2001; Del Rosso et al., 2002). Multiple studies have demonstrated a critical role of matrix metalloproteinases (MMPs) that can degrade the extracellular matrix and basement membrane proteins and facilitate the initial invasion events (Chang and Werb, 2001). Simple inhibition of MMPs, however, is not necessarily beneficial for cancer patients' outcome. The roles of MMPs are quite complex, as they have functions other than promotion of metastasis and have substrates other than extracellular matrix proteins (Egeblad and Werb, 2002). The second, perhaps equally important, group of enzymes involved in degradation of the extracellular matrix and modulation of cell-substratum adhesion is the family of serine proteases (Del Rosso et al., 2002). One of the best-studied serine proteolytic systems at the cell surface is the urokinase-type plasminogen activator (u-PA) and u-PA receptor (u-PAR). The u-PA/u-PAR complex has an intrinsic ability to concurrently regulate pericellular proteolysis and cell surface adhesion receptors.

We present here in vivo evidence that upregulation of type-II cell surface serine protease hepsin leads to disorganization and disruption of basement membrane.

Since hepsin is a serine protease, it is likely that it exercises its function through proteolytic digest of specific substrate proteins. If some of these substrates are the basement membrane proteins, hepsin may be directly involved in degradation of the extracellular matrix. Alternatively, hepsin may activate other proteases that are often synthesized as nonactive proenzymes. By this means, it can activate a proteolytic cascade that will ultimately lead to degradation of the extracellular matrix proteins. Experiments with cultured cell lines demonstrated that

Table 1. Incidence of metastasis in LPB-Tag, PB-Hepsin, and LPB-Tag/PB-Hepsin animals

Genotype	Total # of mice	# of mice with metastasis
LPB-Tag	15	0
PB-Hepsin lines C and D	9	0
LPB-Tag/PB-Hepsin line C	12	5
LPB-Tag/PB-Hepsin line D	20	11

21-week-old mice with indicated genotypes were analyzed by hematoxylin and eosin staining and microscopy. By 21 weeks of age, 55% of LPB-Tag/PB-hepsin line D and 42% of LPB-Tag/PB-hepsin line C animals developed metastases. All LPB-Tag and PB-hepsin mice analyzed were free of metastasis. The differences in metastasis formation between LPB-Tag versus LPB-Tag/PB-hepsin line D and LPB-Tag versus LPB-Tag/PB-hepsin line C animals were statistically significant, with P values of 0.006 and 0.03, respectively.

blood coagulation factor VII may be one of the hepsin proteolytic substrates (Kazama et al., 1995). Hepsin can convert factor VII to VIIa and activate the blood coagulation cascade leading to formation of thrombin, deposition of pericellular fibrin, and activation of PAR-1. Other type II serine proteases have also been demonstrated to be able to activate proteolytic cascades. MT-SP1, a close relative of hepsin, has been shown to activate PAR-2 and pro-u-PA (Takeuchi et al., 2000).

Overexpression of hepsin in metastases-derived human prostate cancer cell lines decreases their ability to invade Laminin 1-based Matrigel (Srikantan et al., 2002). This appears to contradict our findings with in vivo overexpressed hepsin. While the in vitro invasion system is capable of deciphering the differences in the Matrigel degradation abilities, it cannot assay the initial stages of invasion that include disruption of normal epithelial structure, weakening of cell-substratum adhesion, and failure of basement membrane deposition and assembly. Our results demonstrate that hepsin overexpression causes disorganization of the basement membrane and, therefore, is likely to act at the early stages of metastatic pathway. Future experiments will help to determine the substrates for hepsin proteolytic activity that may be responsible for its function in disorganization of the basement membrane.

The type II serine proteases have been previously implicated in cancer progression (Del Rosso et al., 2002; Netzel-Arnett et al., 2003; Wu, 2003). The supporting evidence, however, has been mostly circumstantial. Many of these proteins are upregulated in cancer. For example, corin is upregulated in leimyosarcoma, endometrial carcinoma, and osteosarcoma (Yan et al.,

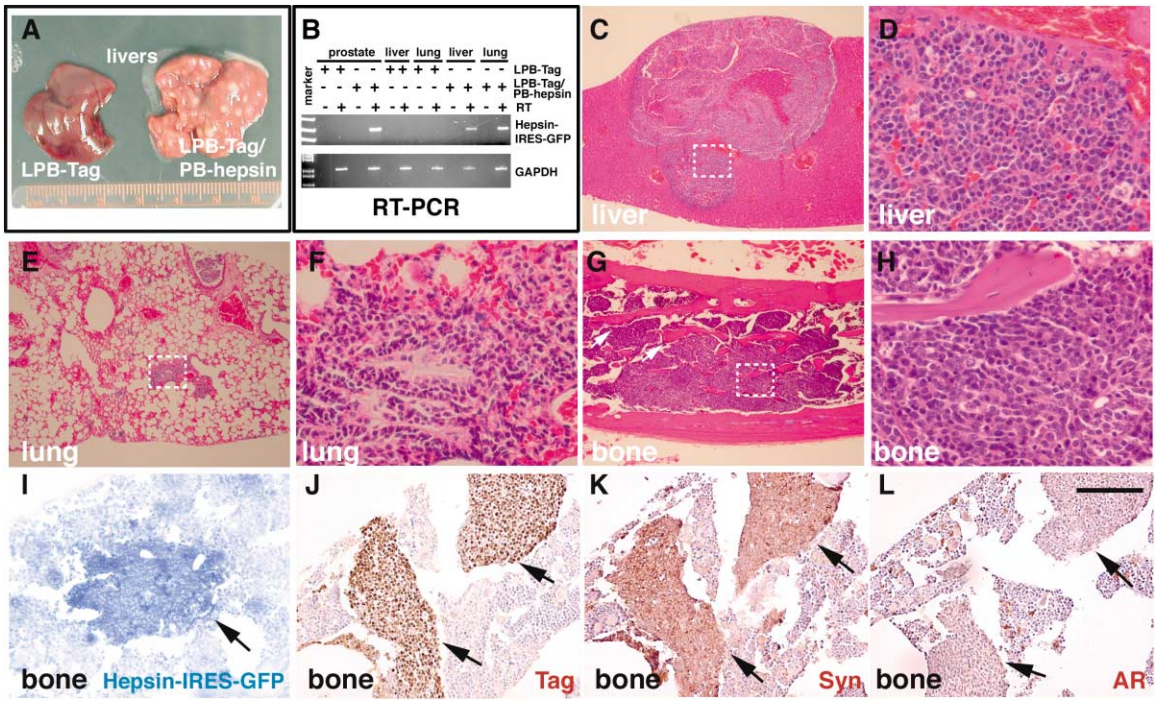

Figure 6. Hepsin promotes metastasis in the LPB-Tag mouse prostate cancer model

A: Macroscopic appearance of livers from 21-week-old LPB-Tag and LPB-Tag/Hepsin animals. Extensive metastasis was observed in double transgenic mice.

B: PB-hepsin transgene expression in prostate metastases to liver and lung from LPB-Tag/PB-hepsin animals. RNA extracted from various organs of LPB-Tag and LPB-Tag/PB-hepsin animals was subjected to RT-PCR analyses with primers specific for PB-hepsin (Hepsin-IRES-GFP) or control GAPDH transcripts. Samples without RT served as controls.

C–H: Histologic appearance of liver (**C** and **D**), lung (**E** and **F**), and bone (**G** and **H**) showing prominent metastases in the LPB-Tag/PB-hepsin mice. Areas within dashed squares of **C**, **E**, and **G** are shown at higher magnification in **D**, **F**, and **H**, respectively.

I–L: Bone metastases in LPB-Tag/PB-hepsin animals are positive for PB-hepsin transgene (Hepsin-IRES-GFP), T-antigen (Tag), synaptophysin (Syn), and androgen receptor (AR) expression. PB-hepsin transgene expression was determined by in situ hybridization (**I**). Expression of T antigen, synaptophysin, and androgen receptor was revealed by immunohistochemistry (**J–L**). The scale bar in **L** corresponds to 0.5 mm in **C**, **E**, and **G**, 0.3 mm in **J–L**, 150 μm in **I**, and 50 μm in **D**, **F**, and **H**.

Table 2. Distant organs displaying metastasis in the LPB-Tag/PB hepsin mice

Genotype of mice with metastasis	Animal #	Organs displaying metastasis				
		Liver	Bone	Lung	Kidney	Spleen
LPB-Tag/PB-hepsin line C	41	+	−	−	−	−
	42	+	+	+	−	−
	57	+	−	+	−	−
	77	+	−	−	−	−
	112	+	+	+	−	−
LPB-Tag/PB hepsin line D	29	+	+	−	−	−
	42	+	+	+	−	−
	43	+	+	−	−	−
	45	−	−	+	−	−
	63	−	−	+	−	−
	71	+	−	+	−	−
	75	+	−	−	−	−
	102	−	+	+	−	−
	133	−	−	+	−	−
	138	+	−	−	−	−
	151	+	−	−	−	−

21-week-old animals were analyzed as described in the legend for Table 1. Only the data for animals with metastasis are shown.

1999). The TMPRSS2 and TMPRSS4 are overexpressed in prostate and pancreatic cancers, respectively (Lin et al., 1999; Wallrapp et al., 2000). Finally, hepsin was found to be overexpressed in prostate and ovarian cancers (Chen et al., 2003; Dhanasekaran et al., 2001; Ernst et al., 2002; Luo et al., 2001; Magee et al., 2001; Stamey et al., 2001; Stephan et al., 2004; Tanimoto et al., 1997; Welsh et al., 2001). Injections of inhibitors of type II serine proteases suppress primary tumor growth and metastasis of human PC3 prostate tumor cells implanted into nude mice (Takeuchi et al., 1999). Tumor cells overexpressing the type II serine protease matriptase show higher incidence of metastasis when they are injected into nude mice (Ihara et al., 2002).

The role of hepsin in prostate cancer has been a matter of debate. While all studies agree that hepsin is upregulated in human prostate cancer, it is not clear how hepsin expression levels correlate with patient outcome. While initially it was found that hepsin levels inversely correlate with the recurrence of prostate cancer (Dhanasekaran et al., 2001), a later study revealed a positive correlation (Stephan et al., 2004). Hepsin overexpression in metastases-derived prostate cancer cell lines decreases their rates of proliferation (Srikantan et al., 2002). Since we found that wild-type mouse prostate epithelial cells do not express endogenous hepsin, it is very difficult to estimate how levels of hepsin expression in our transgenic mice compare to hepsin upregulation in human prostate cancer. The level of expression may play a very important role in the phenotype. If hepsin is involved in degradation of cell-substratum adhesion proteins and its activity is very high, prostate epithelial cells will not be able to maintain substratum adhesion, and will separate from the basement membrane or tissue culture surface and undergo apoptosis. While extracellular matrix degradation is beneficial and sometimes absolutely necessary for initial tumor invasion, it may be less advantageous during the later stages of metastasis formation, where ability to form de novo attachment in distant organs is necessary for metastatic cell survival. It is possible that very high levels of hepsin expression, which are found in a subset of human prostate cancers, may indeed be associated with inhibition of cell growth and better patient survival prognosis. However, moderate levels of upregulation may be sufficient to disrupt the basement membrane and facilitate initial tumor cell spreading, but may not cause complete loss of substratum adhesion and subsequent cell death.

Human prostate cancer metastasizes preferentially to bone. The mechanisms responsible for bone metastasis are not known. Bone metastases are extremely rare in the current mouse models of prostate cancer. Paucity of bone metastases has been one of the major limitations of mouse models of prostate cancer. We demonstrate that, unlike human prostate epithelial cells, mouse prostate epithelium does not express detectable levels of endogenous hepsin. Exogenous transgene expression of hepsin was sufficient to promote prostate cancer metastasis to the bone, as up to 24% of 21-week-old LPB-Tag/PB-hepsin double transgenic animals exhibited bone metastases. It is important to note that these numbers are likely to be an underestimation, since only the femur bones, representing only a small fraction of total bone mass, were analyzed in this study. The bone lesions in the LPB-Tag/PB-hepsin animals do not show obvious osteoblastic or osteolytic characteristics. This is different from human prostate cancer bone metastases that often show osteoblastic characteristics.

Similar to metastatic lesions in other SV40 T antigen-driven mouse models of prostate cancer, metastases in the LPB-Tag/PB-hepsin animals express NE markers. At present, it is not known whether NE markers in these lesions reflect their NE origin, or they emerge during metastatic process as a consequence of epithelial to NE transdifferentiation that may be caused by expression of SV40 T antigen. Since hepsin promotes prostate cancer progression by disorganization of the basement membrane, and disruption of the basement membrane occurs in both NE and non-NE types of prostate cancer, it is likely that hepsin will promote metastasis in the mouse models that do not develop NE differentiation markers. This will be addressed experimentally in our future studies.

Since hepsin promotes prostate cancer progression and metastasis, specific inhibition of hepsin proteolytic activity may be effective in blocking prostate cancer progression in human patients. Hepsin knockout mice have no phenotype (Wu et al.,

1998), suggesting that specific inhibition of hepsin in human patients will not have significant side effects.

In summary, our in vivo studies have revealed a critical role for hepsin in disruption of the basement membrane and promotion of adenocarcinoma and metastasis in a mouse model of prostate cancer. These findings identify hepsin as a metastasis-promoting protein and suggest that it may provide a therapeutic target to prevent metastasis in prostate cancer patients.

Experimental procedures

Plasmids

Generation of PB-IRES-hrGFP transgenic construct

The ARR_2PB synthetic probasin promoter (Zhang et al., 2000) was KpnI(blunted)/SacI digested and subcloned into the NsiI (blunted) and SacI sites of the pIRES-hrGFP-2a vector (Stratagene). The β-globin intron sequence from the K14 expression construct (Vasioukhin et al., 1999) was AvaI (blunted)/NotI digested and subcloned into the SpeI (blunted) and NotI sites of the ARR_2PB-pIRES-hrGFP-2a backbone. The MCS in the pBluescript II KS vector (Stratagene) was modified by SacI/PstI digestion and ligation of oligos encoding the MluI and AscI sites. The ARR_2PB-β-globin-hrGFP-2a-SV40 polyA fragment was ClaI/MluI (partial) digested and subcloned into the ClaI and MluI sites of the modified pBluescript vector. The resulting PB-IRES-hrGFP vector contained the ARR_2PB promoter to direct expression to prostate epithelium, the β-globin intron to increase the levels of the transcript, the multiple cloning site with unique SpeI, NotI, SrfI, XmaI, EcoRI, and SphI cleavage sites for cloning the desired insert, the IRES-hrGFP sequences to reinitiate the translation of the reporter hrGFP from the same transcript, and the SV40 polyadenylation sequence to stabilize the mRNA.

Generation of the PB-hepsin transgenic construct

The full-length mouse hepsin cDNA was PCR amplified from the IMAGE clone #747832 using the primers containing the SpeI and EcoRI sites (5′GCACTAGTATGGCGAAGGAGGGTGGCC3′ and 5′GCGAATTCTCAGG GCTGAGTCACCATG3′). The resulting 1.25 kB fragment was cloned into the SpeI and EcoRI sites of the PB-IRES-hrGFP vector. The PCR-generated hepsin cDNA was verified by sequencing.

Mice

The PB-hepsin fragment was obtained by ClaI/AscI digestion, purified, and injected into fertilized C57BL/6JxCBA mouse eggs. The eggs were transplanted into pseudopregnant females (FHCRC transgenic facility). The resulting mice were screened by PCR with primers used for amplification of the hepsin cDNA in the PB-hepsin plasmid construct (see above). Founder PB-hepsin mice were bred with C57BL/6J animals and the resulting lines were maintained on the C57BL/6J genetic background.

The LPB-Tag mice (line 12-T7f) have been previously described (Kasper et al., 1998). This transgenic line was maintained by breeding with CD-1 animals. LPB-Tag/PB-hepsin double transgenic mice were generated by breeding LPB-Tag females with PB-hepsin males. The resulting double transgenic males were analyzed at 21 weeks of age.

Mouse dissection, internal organ GFP imaging, histology, and electron microscopy

Mice were dissected using the Zeiss SV11 dissecting scope equipped with a GFP attachment. The visible light and GFP images were captured using a Nikon digital camera. The ventral, dorsal, and lateral prostate lobes were dissected and fixed in 4% formaldehyde, processed, and embedded in paraffin. Sections (5 μM) were stained with hematoxylin and eosin, and examined and photographed using a Nikon TE 200 microscope. To study metastasis formation, the liver, lung, kidney, spleen, and femur bone were analyzed. For transmission electron microscopy (EM), samples were fixed in 2% glutaraldehyde, 4% formaldehyde in 0.05M sodium cacodylate buffer at 4°C overnight and processed for Epon embedding. Samples were visualized with a JEOL 1010 microscope.

Northern and Western blot, RT-PCR analyses, and in situ hybridization

Northern and Western blot analyses were carried out according to standard protocols (Sambrook and Russell, 2001). Total RNA was extracted using the Trizol reagent from Gibco. PCR-generated full-length mouse hepsin cDNA and GAPDH probes were used as probes for Northern blot analysis. In situ hybridization was performed on paraffin sections as described previously (Fijnvandraat et al., 2002). The digoxygenin-labeled antisense hrGFP RNA was synthesized using the kit from Roche. The RT-PCR analyses were performed using the kit from Invitrogen. Primers 5′-AGGAGATCATGAGCTT CAAGG-3′ and 5′-GCTGTAGAACTTGCCGCTGT-3′ were used to amplify the transgenic transcript. Primers 5′-CATGTGGGCCATGAGGTCCACCAC-3′ and 5′-TGAAGGTCGGAGTCAACGGATTTGGT-3′ were used to amplify the GAPDH transcript.

Immunofluorescence and immunohistochemistry

For immunofluorescent staining, tissues were embedded in OCT and then frozen immediately on dry ice. The 7 μm cryosections were subjected to indirect immunostaining and analyzed using the Nikon TE 200 microscope equipped with COOLSNAP HQ digital camera or using the Applied Precision, Inc. Delta vision SA3.1 Deconvolution Microscope. In some cases, tissues were first processed, embedded in paraffin, and sectioned, and resulting sections were deparafinized, rehydrated, and processed as described above. The ABC elite or ABC MOM kits (Vector Laboratories) were used for immunohistochemistry. Antibodies were detected with a DAB peroxidase substrate kit and sections were counterstained with hematoxylin QS (both from Vector Laboratories).

Antibodies and apoptosis staining

Antibodies used: anti-hepsin (Cayman Chemical), anti-Collagen I and III (Rockland), anti-β-actin (Sigma), anti-Laminin 5 (β3/γ2 chains), anti-Laminin 1(β1/γ1 chains), anti-fibronectin, anti-β4-integrin (Dr. William Carter, FHCRC), anti-Ki67 (Novacastra Laboratories), anti-keratin 8, anti-Collagen IV (Developmental Studies Hybridoma Bank), anti-keratin 5 (Vasioukhin et al., 2001), anti-synaptophysin (Zymed Laboratories), anti-SV40 T-Ag (Oncogene Research Products), anti-androgen receptor (N-20, Santa Cruz Biotechnology). Relevant FITC- or Texas Red-conjugated donkey or goat antibodies (Jackson Laboratories) were used for detection of primary antibodies. Apoptosis was determined using the FragEL kit from Oncogene Research.

Quantitation of cell differentiation, proliferation, and apoptosis

For quantitation of data obtained using the immunofluorescent stainings, similar areas in the prostates of the PB-hepsin, LPB-Tag, PB-hepsin/LPB-Tag, and wild-type animals were selected, and total number of cells and cells stained positive with indicated antibodies were counted.

Statistical analysis

Fisher's exact test was used to compare the metastases data between the LPB-Tag and LPB-Tag/PB-hepsin animals.

Acknowledgments

We thank Dr. William Carter (Fred Hutchinson Cancer Research Center, Seattle) and Developmental Studies Hybridoma Bank for generous gift of antibodies, Nanyan Jiang for DNA microinjections, Linda Cherepow for help with tissue sectioning, Tania Fernandez for help with mouse genotyping, and Bobbie L. Schneider for help with electron microscopy. We thank Dr. Scott Shappell for confirming the mouse pathology presented. Valeri Vasioukhin is a V Foundation Scholar. This study was supported by the V Foundation for Cancer Research grant, NCI grant R01-CA102365 to V.V., and NCI grants R01-CA76142 and U01 CA84239 and the Frances Williams Preston Laboratories of the T.J. Martell Foundation to R.J.M. J.M. is a recipient of a Department of Defense Postdoctoral Traineeship Award W81XWH-04-1-0050.

Received: May 3, 2004
Revised: June 28, 2004
Accepted: July 1, 2004
Published: August 23, 2004

References

Abate-Shen, C., and Shen, M.M. (2000). Molecular genetics of prostate cancer. Genes Dev. *14*, 2410–2434.

Bernards, R., and Weinberg, R.A. (2002). A progression puzzle. Nature *418*, 823.

Bonkhoff, H. (1998). Analytical molecular pathology of epithelial-stromal interactions in the normal and neoplastic prostate. Anal. Quant. Cytol. Histol. *20*, 437–442.

Chang, C., and Werb, Z. (2001). The many faces of metalloproteases: Cell growth, invasion, angiogenesis and metastasis. Trends Cell Biol. *11*, S37–S43.

Chen, Z., Fan, Z., McNeal, J.E., Nolley, R., Caldwell, M.C., Mahadevappa, M., Zhang, Z., Warrington, J.A., and Stamey, T.A. (2003). Hepsin and maspin are inversely expressed in laser capture microdissectioned prostate cancer. J. Urol. *169*, 1316–1319.

Davis, T.L., Cress, A.E., Dalkin, B.L., and Nagle, R.B. (2001). Unique expression pattern of the $\alpha 6\beta 4$ integrin and laminin-5 in human prostate carcinoma. Prostate *46*, 240–248.

Del Rosso, M., Fibbi, G., Pucci, M., D'Alessio, S., Del Rosso, A., Magnelli, L., and Chiarugi, V. (2002). Multiple pathways of cell invasion are regulated by multiple families of serine proteases. Clin. Exp. Metastasis *19*, 193–207.

Dhanasekaran, S.M., Barrette, T.R., Ghosh, D., Shah, R., Varambally, S., Kurachi, K., Pienta, K.J., Rubin, M.A., and Chinnaiyan, A.M. (2001). Delineation of prognostic biomarkers in prostate cancer. Nature *412*, 822–826.

Egeblad, M., and Werb, Z. (2002). New functions for the matrix metalloproteinases in cancer progression. Nat. Rev. Cancer *2*, 161–174.

Ernst, T., Hergenhahn, M., Kenzelmann, M., Cohen, C.D., Bonrouhi, M., Weninger, A., Klaren, R., Grone, E.F., Wiesel, M., Gudemann, C., et al. (2002). Decrease and gain of gene expression are equally discriminatory markers for prostate carcinoma: A gene expression analysis on total and microdissected prostate tissue. Am. J. Pathol. *160*, 2169–2180.

Fijnvandraat, A.C., De Boer, P.A., Deprez, R.H., and Moorman, A.F. (2002). Non-radioactive in situ detection of mRNA in ES cell-derived cardiomyocytes and in the developing heart. Microsc. Res. Tech. *58*, 387–394.

Hooper, J.D., Clements, J.A., Quigley, J.P., and Antalis, T.M. (2001). Type II transmembrane serine proteases. Insights into an emerging class of cell surface proteolytic enzymes. J. Biol. Chem. *276*, 857–860.

Ihara, S., Miyoshi, E., Ko, J.H., Murata, K., Nakahara, S., Honke, K., Dickson, R.B., Lin, C.Y., and Taniguchi, N. (2002). Prometastatic effect of N-acetylglucosaminyltransferase V is due to modification and stabilization of active matriptase by adding beta 1–6 GlcNAc branching. J. Biol. Chem. *277*, 16960–16967.

Kasper, S., Sheppard, P.C., Yan, Y., Pettigrew, N., Borowsky, A.D., Prins, G.S., Dodd, J.G., Duckworth, M.L., and Matusik, R.J. (1998). Development, progression, and androgen-dependence of prostate tumors in probasin-large T antigen transgenic mice: a model for prostate cancer. Lab. Invest. *78*, 319–333.

Kazama, Y., Hamamoto, T., Foster, D.C., and Kisiel, W. (1995). Hepsin, a putative membrane-associated serine protease, activates human factor VII and initiates a pathway of blood coagulation on the cell surface leading to thrombin formation. J. Biol. Chem. *270*, 66–72.

Lin, B., Ferguson, C., White, J.T., Wang, S., Vessella, R., True, L.D., Hood, L., and Nelson, P.S. (1999). Prostate-localized and androgen-regulated expression of the membrane-bound serine protease TMPRSS2. Cancer Res. *59*, 4180–4184.

Luo, J., Duggan, D.J., Chen, Y., Sauvageot, J., Ewing, C.M., Bittner, M.L., Trent, J.M., and Isaacs, W.B. (2001). Human prostate cancer and benign prostatic hyperplasia: Molecular dissection by gene expression profiling. Cancer Res. *61*, 4683–4688.

Magee, J.A., Araki, T., Patil, S., Ehrig, T., True, L., Humphrey, P.A., Catalona, W.J., Watson, M.A., and Milbrandt, J. (2001). Expression profiling reveals hepsin overexpression in prostate cancer. Cancer Res. *61*, 5692–5696.

Murant, S.J., Handley, J., Stower, M., Reid, N., Cussenot, O., and Maitland, N.J. (1997). Co-ordinated changes in expression of cell adhesion molecules in prostate cancer. Eur. J. Cancer *33*, 263–271.

Nagle, R.B., Hao, J., Knox, J.D., Dalkin, B.L., Clark, V., and Cress, A.E. (1995). Expression of hemidesmosomal and extracellular matrix proteins by normal and malignant human prostate tissue. Am. J. Pathol. *146*, 1498–1507.

Netzel-Arnett, S., Hooper, J.D., Szabo, R., Madison, E.L., Quigley, J.P., Bugge, T.H., and Antalis, T.M. (2003). Membrane anchored serine proteases: A rapidly expanding group of cell surface proteolytic enzymes with potential roles in cancer. Cancer Metastasis Rev. *22*, 237–258.

Robinson, V.L., Kauffman, E.C., Sokoloff, M.H., and Rinker-Schaeffer, C.W. (2004). The basic biology of metastasis. Cancer Treat. Res. *118*, 1–21.

Ryan, M.C., Lee, K., Miyashita, Y., and Carter, W.G. (1999). Targeted disruption of the LAMA3 gene in mice reveals abnormalities in survival and late stage differentiation of epithelial cells. J. Cell Biol. *145*, 1309–1323.

Sambrook, J., and Russell, D.W. (2001). Molecular cloning: A laboratory manual, 3rd ed. (Cold Spring Harbor, N.Y.: Cold Spring Harbor Laboratory Press).

Shappell, S.B., Thomas, G.V., Roberts, R.L., Herbert, R., Ittmann, M.M., Rubin, M.A., Humphrey, P.A., Sundberg, J.P., Rozengurt, N., Barrios, R., et al. (2004). Prostate pathology of genetically engineered mice: Definitions and classification. The consensus report from the Bar Harbor meeting of the Mouse Models of Human Cancer Consortium Prostate Pathology Committee. Cancer Res. *64*, 2270–2305.

Srikantan, V., Valladares, M., Rhim, J.S., Moul, J.W., and Srivastava, S. (2002). HEPSIN inhibits cell growth/invasion in prostate cancer cells. Cancer Res. *62*, 6812–6816.

Stamey, T.A., Warrington, J.A., Caldwell, M.C., Chen, Z., Fan, Z., Mahadevappa, M., McNeal, J.E., Nolley, R., and Zhang, Z. (2001). Molecular genetic profiling of Gleason grade 4/5 prostate cancers compared to benign prostatic hyperplasia. J. Urol. *166*, 2171–2177.

Stephan, C., Yousef, G.M., Scorilas, A., Jung, K., Jung, M., Kristiansen, G., Hauptmann, S., Kishi, T., Nakamura, T., Loening, S.A., and Diamandis, E.P. (2004). Hepsin is highly over expressed in and a new candidate for a prognostic indicator in prostate cancer. J. Urol. *171*, 187–191.

Takeuchi, T., Shuman, M.A., and Craik, C.S. (1999). Reverse biochemistry: Use of macromolecular protease inhibitors to dissect complex biological processes and identify a membrane-type serine protease in epithelial cancer and normal tissue. Proc. Natl. Acad. Sci. USA *96*, 11054–11061.

Takeuchi, T., Harris, J.L., Huang, W., Yan, K.W., Coughlin, S.R., and Craik, C.S. (2000). Cellular localization of membrane-type serine protease 1 and identification of protease-activated receptor-2 and single-chain urokinase-type plasminogen activator as substrates. J. Biol. Chem. *275*, 26333–26342.

Tanimoto, H., Yan, Y., Clarke, J., Korourian, S., Shigemasa, K., Parmley, T.H., Parham, G.P., and O'Brien, T.J. (1997). Hepsin, a cell surface serine protease identified in hepatoma cells, is overexpressed in ovarian cancer. Cancer Res. *57*, 2884–2887.

Vasioukhin, V., Degenstein, L., Wise, B., and Fuchs, E. (1999). The magical touch: Genome targeting in epidermal stem cells induced by tamoxifen application to mouse skin. Proc. Natl. Acad. Sci. USA *96*, 8551–8556.

Vasioukhin, V., Bauer, C., Degenstein, L., Wise, B., and Fuchs, E. (2001). Hyperproliferation and defects in epithelial polarity upon conditional ablation of alpha-catenin in skin. Cell *104*, 605–617.

Wallrapp, C., Hahnel, S., Muller-Pillasch, F., Burghardt, B., Iwamura, T., Ruthenburger, M., Lerch, M.M., Adler, G., and Gress, T.M. (2000). A novel transmembrane serine protease (TMPRSS3) overexpressed in pancreatic cancer. Cancer Res. *60*, 2602–2606.

Welsh, J.B., Sapinoso, L.M., Su, A.I., Kern, S.G., Wang-Rodriguez, J., Moskaluk, C.A., Frierson, H.F., Jr., and Hampton, G.M. (2001). Analysis of gene expression identifies candidate markers and pharmacological targets in prostate cancer. Cancer Res. *61*, 5974–5978.

Werb, Z., Vu, T.H., Rinkenberger, J.L., and Coussens, L.M. (1999). Matrix-degrading proteases and angiogenesis during development and tumor formation. APMIS *107*, 11–18.

Wu, Q. (2003). Type II transmembrane serine proteases. Curr. Top. Dev. Biol. *54*, 167–206.

Wu, Q., Yu, D., Post, J., Halks-Miller, M., Sadler, J.E., and Morser, J. (1998). Generation and characterization of mice deficient in hepsin, a hepatic transmembrane serine protease. J. Clin. Invest. *101*, 321–326.

Yan, W., Sheng, N., Seto, M., Morser, J., and Wu, Q. (1999). Corin, a mosaic transmembrane serine protease encoded by a novel cDNA from human heart. J. Biol. Chem. *274*, 14926–14935.

Zhang, J., Thomas, T.Z., Kasper, S., and Matusik, R.J. (2000). A small composite probasin promoter confers high levels of prostate-specific gene expression through regulation by androgens and glucocorticoids in vitro and in vivo. Endocrinology *141*, 4698–4710.